

Electron emission from clean metal surfaces induced by low-energy light ions

R. A. Baragiola, E. V. Alonso, and A. Oliva Florio

Centro Atómico Bariloche, Comisión Nacional de Energía Atómica, Instituto Balseiro,
Universidad Nacional de Cuyo, 8400 San Carlos de Bariloche, Argentina

(Received 14 March 1978)

We have measured the electron emission yields of clean Li, Al, Cr, Cu, Ag, and Au surfaces under bombardment with H^+ , H_2^+ , D^+ , D_2^+ , and He^+ ions in the energy range 2–50 keV. The clean surfaces were produced by *in-situ* evaporation of high-purity metals under ultrahigh-vacuum conditions. It is found that the Z_2 dependence of the yields for hydrogen and helium projectiles are very similar, that the yields for H^+ and D^+ show the same energy dependence as that of the electronic stopping powers, that molecular ions give lower yields per atom than atomic ions, and that isotope effects are negligible in our energy range. It is proposed that kinetic-electron emission under low-energy-light-ion bombardment results mainly from the escape of excited electrons produced by direct binary collisions between the projectile and the valence electrons of the target.

I. INTRODUCTION

When the surface of a solid body is bombarded by positive ions, electron emission (EE) may be observed. This phenomenon has received a great deal of attention in the past¹ because its understanding is essential for adequate measurements of ion currents, the use of particle multipliers, and the proper interpretation of gas discharges, plasma surface interactions (like in a controlled thermonuclear reactor), and electrical breakdown. Furthermore, the study of EE can provide a more detailed picture of the inelastic processes which occur during the passage of atomic particles through matter than is possible through measurements of stopping powers and can also give information on the electronic structure of surfaces. It is regretful therefore, that the vast majority of experimental work done in this field for nearly 80 years concerns poorly controlled surface conditions and hence cannot be clearly interpreted.

EE from solids under ion bombardment can proceed by two distinguishable mechanisms. For ion velocities below about 10^7 cm/sec, ejection of electrons will occur primarily by the potential or Auger mechanism provided that the energy released in the neutralization of the positive ion exceeds twice the work function of the solid. This mechanism was first proposed by Holst and Oosterhuis² and examined in detail by Hagstrum³ who showed that the measurement of electron energy distributions produced by very slow ions is one of the most powerful tools in the study of the electronic structure of surfaces—the technique of ion-neutralization spectroscopy,⁴ the solid-state analog of Penning-ionization-electron spectroscopy devised by Cermák⁵ and used in molecular physics.

Ions with higher velocities eject electrons by the

so-called “kinetic” mechanism in which electrons may be accelerated as a result of collisions between the projectile and lattice atoms or from direct “binary” collisions between the ion and nearly free valence-band electrons. At velocities larger than the Fermi velocity of target electrons, another process becomes important. The projectile will then be able to excite efficiently surface and bulk plasmons which decay mainly through the creation of an electron-hole pair; the electrons may then be ejected into vacuum with a maximum energy equal to the plasmon energy minus the work function.

Most of the measurements performed with clean surfaces were for the energy range where the potential mechanism predominates. This is especially so for light particles, which are very inefficient in removing adsorbed layers by sputtering so one must rely on different cleaning techniques and the use of ultrahigh vacuum (UHV) (pressures less than 10^{-8} Torr). So there are only very few measurements for light particles like H^+ and He^+ in the region where the kinetic mechanism is more important, which is unfortunate since this type of data is needed in the field of nuclear fusion.

In this paper we report on measurements of electron yields γ (average number of electrons released per incident particle) for 2–50-keV H^+ , H_2^+ , D^+ , D_2^+ , and He^+ projectiles on clean targets of Li, Al, Cr, Cu, Ag, and Au. The measurements were performed at background pressures in the 10^{-10} -Torr range and the surfaces were prepared by *in-situ* evaporation of high-purity metals.

II. APPARATUS

The apparatus used in this work is shown schematically in Fig. 1. Basically, it consists of an ion accelerator with mass selector, a beam steering

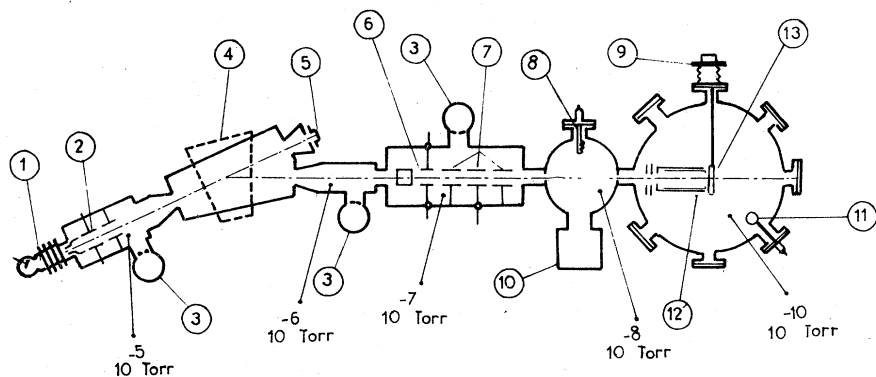


FIG. 1. Experimental apparatus. 1—rf ion source, 2—focusing lens, 3—diffusion pump, 4—mass-sorting magnet, 5—Faraday cup, 6—steering plates, 7—Einzel lens, 8—titanium sublimator, 9—manipulator, 10—ion pump, 11—quartz-crystal resonator, 12—collector assembly, and 13—target.

and focusing stage, a differential-pumping stage, and an UHV target chamber.

The purpose of the differential-pumping stage is to minimize the flow of gases into the target chamber. The operating pressure in this stage is kept at $\sim 10^{-8}$ Torr by ion and Ti-sublimation pumping. The design is such that oil from the accelerator (pumped by diffusion pumps) cannot creep into the UHV chamber without first encountering a water-cooled Ti-covered surface. The solid angle for direct line-of-sight gas flow from the previous stages to the target is less than 10^{-5} sr. Therefore, the impingement rate of molecules from these stages on the target will be $\sim 10^9$ mol/cm² sec,⁶ and small compared to that from the background UHV environment.

The target chamber is constructed of bakeable materials and pumped by an ion and a Ti-sublimation pump. During Ti-sublimation, the target is moved into a N₂-liquid-cooled shield to prevent its surface from contaminating with Ti. Base pressures are in the range 5×10^{-11} – 5×10^{-10} Torr and consist typically of 70% H₂, the remaining being mostly CO and CH₄. The operating pressure with the ion beam on was always kept in the 10^{-10} -Torr range.

The target and collector assembly are shown in detail in Fig. 2. The ion beam is collimated by the 1.5-mm-diam apertures *D1* and *D2* which together with apertures in the differential-pumping stage restrict the angular divergence of the beam to $\sim 0.2^\circ$ and so prevent it from hitting surfaces other than the target. The halo stripper *D3* is used to avoid that particles scattered from *D2*, hit the suppressor or the collector. The suppressor is held at a sufficiently negative voltage so as to prevent electrons coming from the previous apertures to reach the target or the collector and also to prevent electrons emitted from the target to escape the collector. The voltage chosen -200 V was substantially above the saturation value, defined as the voltage at which the current measured

in the collector is within 1% of the asymptotic value obtained at higher voltages. The target is mounted on a manipulator which allows it to be moved away from the collector and then rotated 90° to face the evaporation source used to produce the clean metal surfaces. As a consequence of the geometry shown in Fig. 2, all the values of γ being reported here refer to normal incidence of the ions to the surface.

III. EXPERIMENTAL PROCEDURE

A. Beam-energy calibration

In order to investigate the existence of isotope and molecular effects it is important to know accurately the energy of the ion beam. This energy is given by the charge of the ions times the applied acceleration voltages (accelerator plus postacceleration at the target) plus the excess energy due to the plasma potential in the ion source.⁷ This last contribution was determined to be 110 ± 30 eV for our working conditions in the rf ion source. The overall accuracy of the beam energy measurement was $\pm (0.1\% + 30 \text{ eV})$.

B. Current measurements

The circuit used for taking data is shown in Fig. 2. During measurements of electron yields γ , the

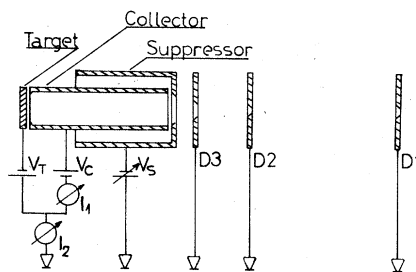


FIG. 2. Schematic drawing of the collimators and the target-collector assembly.

voltages applied to target and collector where -90 and $+30$ V, respectively, with respect to ground. This 120-V potential was about twice that required to achieve saturation in the electron current to within 1%. The quantity $I = I_1/I_2$ is the normalized electron current, I_1 being the current on the collector and I_2 the total current entering the target-collector system. The current I_1 is equal to $I_e + I_{ni} - I'_{pi}$ where I_e is the electron current, I_{ni} the current of negative secondary ions (reflected and sputtered) and I'_{pi} the current of positive secondary ions with energy larger than $120q$ eV where q is the charge of these ions. For clean targets, the secondary ion current corresponds to backscattered ions essentially, and is known to be two orders of magnitude smaller than the electron emission current from measurements by Fogel *et al.*⁸ for light ions in Mo in our energy range. For other materials we can integrate existing data of energy distribution of neutral and charged backscattered particles^{9, 10} to obtain relative backscattered ion yields which can be converted to absolute values using data on total (ions plus neutrals) backscattering yields.¹¹ In all cases considered, the yields of backscattered ions were found to be less than 2% of the electron yields. Therefore $\gamma = I_1/I_2$ within our experimental uncertainties of 4%.

One source of error which is present in many old investigations and which was tried to minimize in this one is caused by the existence of energetic neutrals in the beam, formed by electron capture collisions with the background gas, along the path between the analyzing magnet and the target. Neutral atoms will not contribute to the measured ion current but will nevertheless eject electrons from the target. In our case the effect of neutrals on the measurements was less than 2%. This was determined by deflecting the ion beam at the entrance of the UHV chamber by an externally applied magnetic field while recording the electron current on the collector.

C. Target preparation and cleaning

In past investigations on ion-EE,¹ the generation of clean surfaces was attempted by two methods, heating to high temperatures and cleaning by inert gas ion sputtering. Heating has the drawbacks that for most materials, nonvolatile surface compounds are present which cannot be removed by heating alone¹² and that bulk impurities may diffuse and accumulate on the surface at high temperatures.^{10, 13} On the other hand, sputtering by inert gas ions, the standard cleaning technique used nowadays in surface studies, has been found to be satisfactory in studies of EE.¹⁴ A third technique

was used mainly in this work in which clean surfaces were produced by *in-situ* evaporation in UHV of high-purity (better than 99.9%) materials. In order to minimize contamination of the target by trapped ions when bombarding with hydrogen beams, doses used for obtaining a data point (average of several measurements) were kept low ($< 10^{13}$ ions/cm²).

D. Measuring procedure

Immediately after obtaining a clean surface, γ was measured using 30-keV Ar⁺ projectiles and its invariance with ion dose, verified. Measurements of the yields for each ion as a function of energy was then performed, starting at the highest energy. After this, the high-energy measurements were made again. Whenever results were not reproduced, indicating that adsorption of residual gas was significant, a clean surface was prepared again either by a new evaporation or by sputtering, and measurements conducted again.

Care was taken not to use deuterium immediately after a hydrogen run, to avoid contamination of the D⁺ beam with H₂⁺ ions produced in the ion source from residual hydrogen trapped in its walls. The inverse situation was also avoided in order not to contaminate the H₂⁺ beam with D⁺ ions. After working with He and Ar for a few minutes, it was found that hydrogen or deuterium impurity peaks in the mass spectrum were negligible. D₂⁺ contamination in the He⁺ beam was also negligible as inferred from the observed low abundances of ions with mass to charge ratios of 2 (D⁺ or H₂⁺, also He²⁺) and mass 6 (D₃⁺) ions.

IV. RESULTS

The experimental results are shown in Figs. 3-8 as a function of projectile velocity. Interpolated values are shown in Table I, as a function of ion energy. Total errors which include statistical uncertainties and systematic errors from the measuring instruments, neglect of backscattered ions and presence of neutrals in the beam are $\pm 4\%$.

No evidence for isotope effects in the yields of H⁺ (H₂⁺) ions as compared with those of equal velocity D⁺ (D₂⁺) was observed within experimental errors, in our velocity range. This does not rule out the possibility of isotope effects at very low velocities where the energy degradation, energy, and angular straggling of the ions over the effective electron escape depths are important, since these effects show a mass dependence.¹

The results for molecular ions are presented divided by two as is common practice and so they represent electron yields per atom. These reduced yields were always found to be less than

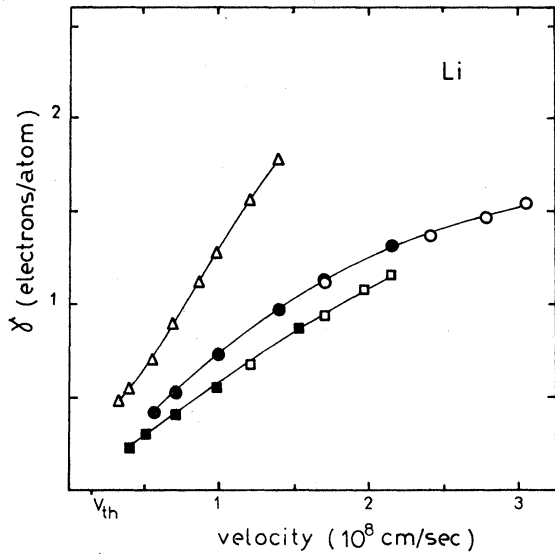


FIG. 3. EE yields per atom from lithium targets vs the velocity of the projectiles. \circ — H^+ , \bullet — D^+ , \square — H_2^+ , \blacksquare — D_2^+ , \triangle — He^+ . V_{th} is given by Eq. (2) in text.

that for atomic particles at equal velocities due to the smaller value of the potential EE yields for molecules than for atomic ions¹⁵ and to interference effects in the excitation of target electrons by the correlated constituents of the molecular ion.¹⁶

Results obtained by other workers are also shown in Figs. 3–8 for comparison. The only data shown are from papers where it is stated that some effort was made to keep the surfaces reason-

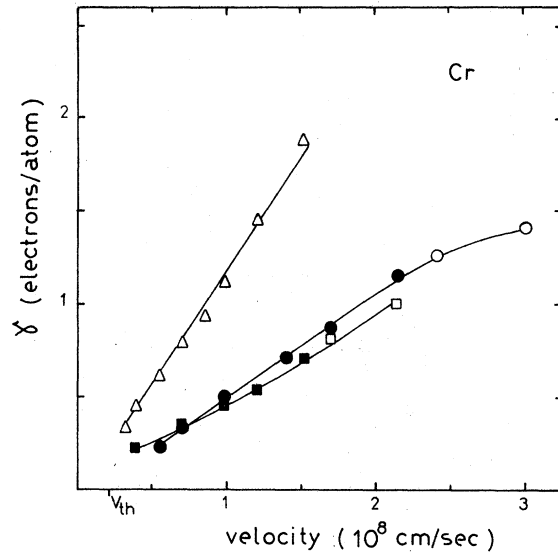


FIG. 5. EE yields per atom from chromium targets vs the velocity of the projectiles. \circ — H^+ , \bullet — D^+ , \square — H_2^+ , \blacksquare — D_2^+ , \triangle — He^+ . V_{th} is given by Eq. (2) in text.

ably clean, either by sputtering with a high current density beam (in the case of He projectiles) or by heating before or during bombardment while keeping the background pressure low. The results of Losch¹⁷ for H_2^+ on Al are in fair agreement with ours. This worker cleaned his surfaces by sputtering in an Ar discharge and conducted measure-

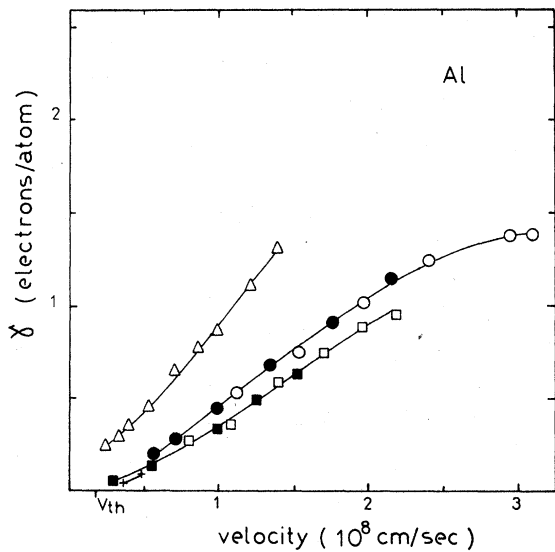


FIG. 4. EE yields per atom from aluminum targets vs the velocity of the projectiles. \circ — H^+ , \bullet — D^+ , \square — H_2^+ , \blacksquare — D_2^+ , \triangle — He^+ , this work. +—from Losch (Ref. 17) for H_2^+ . V_{th} is given by Eq. (2) in text.

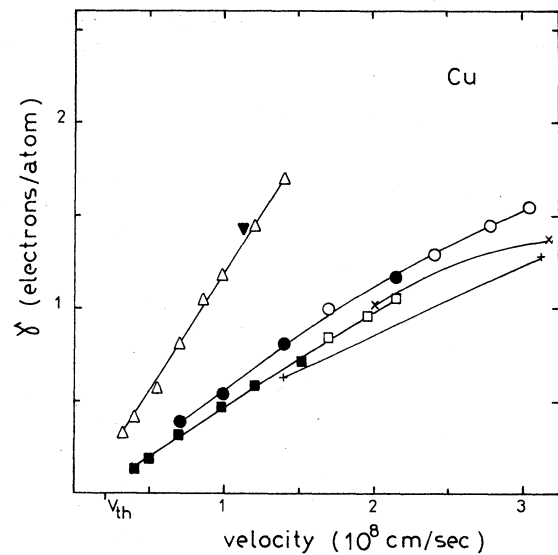


FIG. 6. EE yields per atom from copper targets vs the velocity of the projectiles. \circ — H^+ , \bullet — D^+ , \square — H_2^+ , \blacksquare — D_2^+ , \triangle — He^+ , this work. \times — H^+ , $+$ — H_2^+ from Large and Whitlock (Ref. 18), \blacktriangledown — He^+ from Evdokimov *et al.* (Ref. 19). V_{th} is given by Eq. (2) in text.

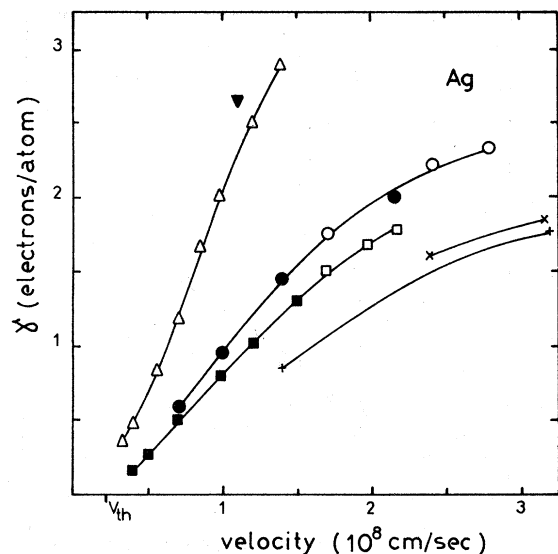


FIG. 7. EE yields per atom from silver targets vs the velocity of the projectiles. \circ — H^+ , \bullet — D^+ , \square — H_2^+ , \blacksquare — D_2^+ , Δ — He^+ , this work. \times — H^+ , $+$ — H_2^+ from Large and Whitlock (Ref. 18), \blacktriangledown — He^+ from Evdokimov *et al.* (Ref. 19). V_{th} is given by Eq. (2) in text.

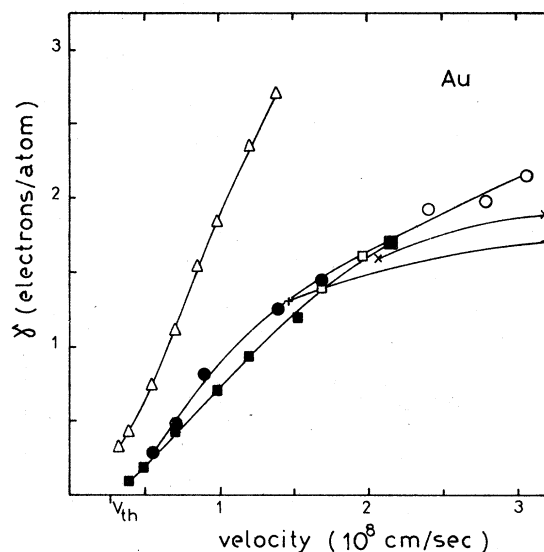


FIG. 8. EE yields per atom from gold targets vs the velocity of the projectiles. \circ — H^+ , \bullet — D^+ , \square — H_2^+ , \blacksquare — D_2^+ , Δ — He^+ , this work. \times — H^+ , $+$ — H_2^+ from Large and Whitlock (Ref. 18). V_{th} is given by Eq. (2) in text.

ments at 10^{-8} Torr. Since at these pressures, gas adsorption occurs rapidly, Losch measured γ as a function of time and extrapolated the results to zero times.

The results of Large and Whitlock¹⁸ for H^+ and

H_2^+ on Cu, Ag, and Au are somewhat lower than ours. These workers attempted to clean their targets by flashing to temperatures 10–80°K below the melting point for each material. As stated above, the net result of this is the diffusion of bulk impurities to the surface.^{10, 13} Furthermore, they

TABLE I. Electron yields per atom for H^+ , H_2^+ , and He^+ ions on Li, Al, Cr, Cu, Ag, and Au, obtained by graphical interpolation between data points.

Target	Projectile	Energy (keV)									
		2	3	4	7	10	15	20	30	40	50
Li	H^+	0.475	0.560	0.650	0.830	0.965	1.12	1.23	1.36	1.46	1.55
	H_2^+	0.260	0.320	0.365	0.465	0.550	0.680	0.775	0.945	1.07	1.16
	He^+	0.465	0.525	0.590	0.740	0.880	1.10	1.27	1.54	1.77	1.95
Al	H^+	0.225	0.310	0.380	0.560	0.700	0.875	1.01	1.23	1.34	1.38
	H_2^+	0.087	0.132	0.156	0.230	0.310	0.450	0.555	0.745	0.885	0.955
	He^+	0.280	0.330	0.380	0.510	0.620	0.765	0.885	1.10	1.31	...
Cr	H^+	0.280	0.360	0.430	0.580	0.710	0.880	1.04	1.26	1.36	1.42
	H_2^+	0.240	0.270	0.305	0.375	0.450	0.540	0.635	0.810	0.940	1.01
	He^+	0.310	0.420	0.485	0.650	0.780	0.960	1.10	1.42	1.69	1.94
Cu	H^+	...	0.420	0.480	0.650	0.780	0.960	1.08	1.29	1.45	1.57
	H_2^+	0.162	0.210	0.265	0.380	0.470	0.580	0.670	0.830	0.960	1.08
	He^+	...	0.390	0.455	0.620	0.800	1.04	1.18	1.44	1.70	...
Ag	H^+	...	0.650	0.810	1.15	1.42	1.70	1.89	2.17	2.33	...
	H_2^+	0.225	0.295	0.375	0.610	0.800	1.03	1.20	1.50	1.67	1.78
	He^+	0.360	0.450	0.570	0.910	1.21	1.65	2.00	2.50	2.89	...
Au	H^+	0.360	0.540	0.680	0.980	1.22	1.46	1.64	1.77	2.03	2.15
	H_2^+	0.138	0.240	0.325	0.550	0.720	0.930	1.09	1.38	1.59	1.70
	He^+	0.315	0.410	0.510	0.810	1.09	1.52	1.83	2.34	2.68	...

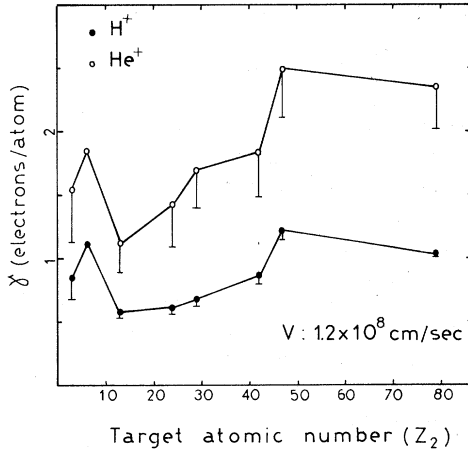


FIG. 9. Electron yields γ vs Z_2 , the atomic number of the target atoms for a fixed value of the velocity of the projectiles, $v = 1.2 \times 10^8$ cm/sec. The bars indicate the values of the potential emission yields in the limit of zero velocity, as given by Kishinevskii (Ref. 21). ϵ data from Ref. 26.

worked at pressures of $(1-2) \times 10^{-8}$ Torr and admit that during their measurement time the surfaces became covered with about a monolayer of adsorbed gas.

Data of Evdokimov *et al.*¹⁹ for He^+ on Cu and Ag are the same as ours within combined experimental errors. These workers used intense ion beams of a few hundred $\mu\text{A}/\text{cm}^2$ and residual pressures were in the 10^{-7} -Torr range.²⁰ It seems from the agreement with our results that the rate of removal of contaminants by sputtering was much larger than the rate of their arrival from the background gas.

Figure 9 shows that the Z_2 dependences of γ for H^+ (D^+) and He^+ ions at the constant velocity $v = 1.2 \times 10^8$ cm/sec are similar. The bars give the magnitude of the potential emission coefficient in the limit of low velocities obtained using Kishinevskii's formula.²¹ It must be pointed out, however, that the points lying at the lower end of the bars need not correspond to pure kinetic emission since (i) Kishinevskii's model has many simplifying assumptions and (ii) the actual magnitude of potential emission yields γ_p are unknown at this velocity and so far the approximate independence of γ_p with ion velocity has been tested only up to $v = 5 \times 10^7$ cm/sec for He^+ ,²² and Ne^+ and Ar^+ projectiles.²³

V. THEORY AND DISCUSSION

In the case of He^+ projectiles, potential emission contributes substantially to the yields in our energy range, due to the large ionization energy of He .^{3, 21, 22} Present theories of potential emission^{3, 21} hold for very low particle velocities where ion penetration in the solid is negligible, and are not,

therefore, applicable to our work. We will then concentrate to the case of incident protons and deuterons where, except for Li targets, kinetic emission is clearly predominant in our velocity range.

Existing theories of kinetic ion EE have been discussed by Arifov.¹ In our low velocity range he considers the theory of Parilis and Kishinevskii²⁴ or their modifications for light ions²⁵ to give a correct description of reality. These theories assume that EE results from the following mechanism. As a result of violent binary collisions between the projectile and lattice atoms, holes are created in the core levels of the latter. These holes are then filled by Auger processes and if the condition $\delta > 2\phi$ is fulfilled, electrons may be ejected into vacuum. Here δ is the binding energy of electrons in the core level relative to vacuum and ϕ the work function of the solid.

We will not enter at this point into a detailed discussion of this model. This will be done in a future publication.²⁶ For the purpose of the present work it will be sufficient to estimate the importance of this mechanism. Let us consider the case of proton impact on aluminium for which data are available²⁷ for the cross section for L -shell ionization. The measured cross sections rise from $\sim 8 \times 10^{-19}$ cm^2/atom at 15 keV to $\sim 7 \times 10^{-18}$ cm^2/atom at 50 keV. Not only are the cross sections very low but their energy dependence is clearly not contained in the experimental electron yield curves (in the same energy range γ increases only a factor ~ 1.6). Analogous situations should be expected for the tightly bound electrons of the other targets.

There remains the possibility of exciting the more loosely bound electrons of the target. Let us first consider the case in which valence electrons may be considered to behave as a free electron gas. This assumption should be quite reasonable for metals like Li and Al. In this approximation we will neglect phonon-assisted umklapp processes which are known to be relatively unimportant from the theory of electron-induced secondary EE.^{28, 29} Electron excitation will then result in this model from the screened Coulomb interaction between the projectile and the target electrons through direct binary collisions and the decay of collective excitations (plasmons). At velocities smaller than v_F , the velocity of the electrons at the Fermi surface, plasmons will be excited inefficiently. The threshold velocity for ejection of an electron into vacuum v_{th} , will be that at which the maximum energy transfer equals the work function, that is,

$$2 m v_{th} (v_{th} + v_F) = \phi, \quad (1)$$

$$v_{th} = \frac{1}{2}v_F [(1 + 2\phi/mv_F^2)^{1/2} - 1]. \quad (2)$$

At v_{th} the electron emission yield should vanish since the excited electron will be traveling in the direction of incidence of the projectile and in order to revert its motion towards the surface it will need to undergo collisions. These collisions will of necessity take some kinetic energy from the electron and force it to sink below the vacuum level. In any real solid, however, umklapp processes which were neglected at high velocities will be relatively important at these low velocities, and the absolute threshold will be determined from energy conservation alone, resulting in

$$V_{th}^{abs} = (2\phi/M)^{1/2}$$

or

$$E_{th}^{abs} = \frac{1}{2}M(V_{th}^{abs})^2 = \phi, \quad (3)$$

where M is the mass of the bombarding ion. This case will be analogous to the surface effect in secondary and photoelectric emission.²⁹

The threshold velocities predicted in the free-electron model [Eq. (2)] are shown in Figs. 4-9 and they can be seen to be consistent with extrapolation of the experimental results, except for Li which gives high potential emission yields due to its low work function.

At velocities not too close to v_{th} we can expect, in analogy with ionization in gases and semiconductors, that the mean energy which the projectile must spend in creating an electron-hole pair, J (with the final electron energy lying above the vacuum level) is independent of the ion velocity.³⁰ Therefore, the number of excited electrons generated by the incident ion of energy E_0 in a layer of thickness dx at a depth x below the surface will be

$$n(x, E)dx = (1/J)S_e(x, E), \quad (4)$$

where $S_e = (dE/dx)_e$ is the electronic stopping power of the solid for the projectile, and E the projectile energy at depth x .

The excited electrons will then diffuse in the solid scattering against other electrons, defects and phonons, with a certain mean free path to be "absorbed," that is to be degraded in energy to be below the vacuum level. The mean free paths which are a function of electron energy have so far been calculated using very simple models of the solid which do not include any band-structure effects.^{31,32} The net effect of averaging the transport of electrons to the surface over electron energies and paths is usually approximated by the attenuation function $f(x) = \frac{1}{2}\exp(-x/L)$ for normal incidence of the projectile³³ where the factor $\frac{1}{2}$ takes into account that in the cascade there are equal number of electrons moving in the forward that in the back-

ward hemisphere (forward is the direction of the incident ion) and where L is a mean attenuation length which will be shorter than the average mean free path $\langle \lambda \rangle$ since the excited electron will certainly not follow the shortest route from the interior of the solid to the surface.

Once the electron reaches the surface, it must overcome the surface potential barrier in order to escape into vacuum. The average escape probability P resulting from integration over all electron energies and angles of incidence to the surface has again been calculated only for very simple models of the solid. The results are very sensitive to the choice of the barrier height, which in the Sommerfeld model is $E_F + \phi$, where E_F is the Fermi energy. For real solids, the barrier height will depend strongly on the detailed form of the band structure. Furthermore, surface umklapp processes³⁴ need to be considered and a quantum mechanical calculation of P will be required since the wavelengths associated with the excited electrons are of the order of the width of the barrier.

Due to the difficulties of evaluating each parameter for any given case, we will not attempt to make a detailed theory at this stage. The elementary semiempirical model developed above gives

$$\gamma = P \int_{\infty}^0 n(x, E) f(x) dx = \frac{P}{2J} \int_0^{\infty} S_e(x, E) e^{-x/L} dx, \quad (5)$$

which is essentially the same as that derived for secondary EE under electron bombardment.^{33,35} In our case, we can expect Eq. (5) to be more accurate than for electron bombardment since in the latter case a large correction due to backscattered projectiles must be made³⁶ while in ion-electron emission such correction will be small, except at very low projectile velocities. In the case of heavy particles and specially if $M_1 > M_2$, where M_1 and M_2 are the masses of projectile and target atoms, respectively, a correction to Eq. (5) will be required to take into account the generation of excited electrons by recoiling target atoms.

At velocities not too close to the threshold [Eq. (2)], the projectiles will lose a very small fraction of their energy over the mean electron escape depth. We can then take the stopping power outside the integral in Eq. (5) and obtain

$$\gamma(E_0) = \frac{1}{2}PLS_e(E_0)/J, \quad (5')$$

with the important consequence that γ should have the same energy dependence as the electronic stopping power, as proposed by Bethe³⁷ and used by Sternglass³⁸ for describing ion-electron emission at high velocities. The validity of this conclusion

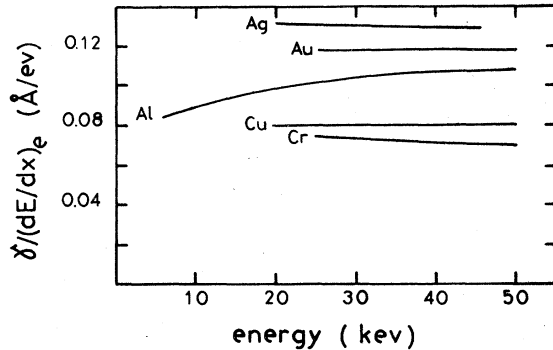


FIG. 10. Ratios between the electron yields γ and the electronic stopping power $(dE/dx)_e$ vs H^+ energy. The curves are derived from smooth fits to our data and to stopping power data (Ref. 39). $(dE/dx)_e$ value for Al at low energies may have errors due to the existence of surface oxide layers in the very thin foils used in the experiments.

can be tested by plotting $\gamma(E_0)/S_e(E_0)$ versus ion energy. This has been done using our measured electron yields and published data³⁹ of S_e for the case of hydrogen ions. Figure 10 shows that these ratios are indeed constant within the experimental uncertainties in γ and S_e , and therefore confirm the validity of Eq. (5') in our energy range.

A model similar to this one has been recently published by Beuhler and Friedman.⁴⁰ The main difference is that they assume that the number of excited electrons is proportional to $S_e(E)$ [our Eq. (4)] at any value of the projectile energy. They take into account the slowing down of the projectiles within the electron escape depth, which is important at low velocities but assume no backscattering of the projectiles and straight line trajectories during penetration. At low velocities, these two assumptions and the use of a constant J value limit the validity of their model. Measurements of the electron yields at very low energies using ground state H or He atoms would test the range of validity of Eq. (4) and provide a better indica-

tion on the existence of a threshold velocity [Eq. (2)] than is possible through the results presented here.

VI. CONCLUSIONS

We have studied the EE from clean metal surfaces under light ion bombardment at keV energies. We have found that for H^+ and D^+ ions, electron yields for each element have the same energy dependence as the corresponding electronic stopping power, thus confirming an idea put forward by Bethe.

It is proposed that the main mechanism for kinetic EE from metals by light ions is the direct screened Coulomb binary interaction between the projectiles and valence-band electrons and the subsequent diffusion and escape of those electrons into vacuum. The mechanism should operate above a threshold value of the projectile velocity which is of the order of 2×10^7 cm/sec. The presence of umklapp processes should result in an absolute threshold energy equal to the work function of the solid.

Electron yields for H^+ and He^+ have a similar Z_2 dependence which is, however, of different nature than the Z_2 dependence of electronic stopping powers, meaning that the processes of electron transport and escape vary substantially among different metals.

ACKNOWLEDGMENTS

The authors are grateful to Dr. O. Auciello and Dr. G. Lantschner for their help in the early part of this work and to Lic. J. Ferrón and Ing. H. Raiti for their help during the experiments. One of us (R. A. B.) would like to thank Dr. I. N. Evdokimov for useful discussions and Dr. Benazeth for helpful conversations about the results of Ref. 31. This work was supported in part by the IAEA under Contract No. 1928/RB and by the Multinational Program in Physics of the Organization of American States.

¹For reviews see: M. Kaminski, *Atomic and Ionic Impact Phenomena on Metal Surfaces* (Springer-Verlag, Berlin; 1965); D. B. Medved and I. S. Strasser, *Adv. Electron. Electron Phys.* **21**, 101 (1965); I. A. Abroyan, M. A. Ereemeev, and N. N. Petrov, *Usp. Fiz. Nauk* **92**, 105 (1967) [*Sov. Phys.-Usp.* **10**, 332 (1967)]; K. H. Krebs, *Fortschr Phys.* **16**, 419 (1968); G. Carter and J. S. Colligon, *Ion Bombardment of Solids* (Heinemann, London, 1968); U. A. Arifov, *Interaction of Atomic Particles with a Solid Surface* (Consultants Bureau, New York, 1969); G. M. McCracken, *Rep. Prog. Phys.* **38**, 241 (1975).

²G. Holst and E. Oosterhuis, *Physica (Utr.)* **1**, 82 (1921).

³H. D. Hagstrum, *Phys. Rev.* **96**, 325 (1954); **96**, 336 (1954); **122**, 83 (1961); H. D. Hagstrum and Y. Takeishi, *ibid.* **137**, A304 (1965); H. D. Hagstrum, Y. Takeishi, and D. D. Pretzer, *ibid.* **139**, A526 (1965); H. D. Hagstrum and G. E. Becker, *Phys. Rev. B* **8**, 107 (1973).

⁴H. D. Hagstrum, *Phys. Rev.* **150**, 495 (1966); *J. Vac. Sci. Technol.* **12**, 7 (1975).

⁵V. Cermák, *J. Chem. Phys.* **44**, 3774 (1966).

⁶E. V. Kornelsen and B. Domeij, *J. Vac. Sci. Technol.* **3**, 20 (1966).

⁷C. J. Cook, O. Heinz, D. C. Lorents, and J. R. Peter-

- son, *Rev. Sci. Instrum.* **33**, 649 (1962). Our rf ion source is of different type and does not use a magnetic field; therefore their results are not directly comparable with ours.
- ⁸Ya. M. Fogel', R. P. Slabospitskii, and A. B. Rastrepin, *Zh. Tekh. Fiz.* **30**, 63 (1960) [*Sov. Phys. Tech. Phys.* **5**, 58 (1960)].
- ⁹P. Meischner and H. Verbeek, *J. Nucl. Mater.* **53**, 276 (1974).
- ¹⁰W. Eckstein and F. E. P. Matschke, *Phys. Rev. B* **14**, 3231 (1976).
- ¹¹O. S. Oen and M. T. Robinson, *J. Nucl. Mater.* **63**, 210 (1976).
- ¹²R. C. Bradley, *J. Appl. Phys.* **30**, 1 (1959); E. Ruedl and R. C. Bradley, *J. Phys. Chem. Solids* **23**, 885 (1962); J. A. McHugh and J. C. Sheffield, *J. Appl. Phys.* **35**, 512 (1964).
- ¹³H. E. Farnsworth, R. E. Schlier, T. H. George, and R. M. Burger, *J. Appl. Phys.* **29**, 1150 (1958); H. D. Hagstrum and C. D'Amico, *ibid.* **31**, 715 (1960); D. W. Vance, *Phys. Rev.* **164**, 372 (1967); L. A. Harris, *J. Appl. Phys.* **39**, 1428 (1968); N. J. Taylor, *Surf. Sci.* **15**, 169 (1969); E. N. Sickafus, *ibid.* **19**, 181 (1970); T. Smith, *ibid.* **27**, 45 (1971).
- ¹⁴H. D. Hagstrum, *Phys. Rev.* **119**, 940 (1960).
- ¹⁵F. M. Propst and E. Lüscher, *Phys. Rev.* **132**, 1037 (1963).
- ¹⁶R. A. Baragiola, E. V. Alonso, A. Oliva Florio, and G. Lantschner, *Abstracts of the Seventh International Conference on Atomic Collisions in Solids* (Moscow State University, Moscow, 1977), p. 350.
- ¹⁷W. H. P. Losch, *Phys. Status Solidi A* **2**, 123 (1970).
- ¹⁸L. N. Large and W. S. Whitlock, *Proc. Phys. Soc.* **79**, 148 (1962).
- ¹⁹I. N. Evdokimov, E. S. Mashkova, V. A. Molchanov, and D. D. Odintsov, *Phys. Status Solidi* **19**, 407 (1967).
- ²⁰I. N. Evdokimov, private communication to one of us (R.A.B.).
- ²¹L. M. Kishinevskii, *Radiat. Eff.* **19**, 23 (1973).
- ²²U. A. Arifov, R. R. Rakhimov, and Kh. D. Dzhurakulov, *Radiotekh. Élektron.* **8**, 223 (1963) [*Radio Eng. Electr.* **8**, 260 (1963)].
- ²³M. Perdrix, S. Paletto, R. Goutte, and C. Guillaud, *Phys. Lett. A* **28**, 534 (1969).
- ²⁴E. S. Parilis and L. M. Kishinevskii, *Fiz. Tverd. Tela* **3**, 1219 (1961) [*Sov. Phys.-Solid State* **3**, 885 (1961)].
- ²⁵L. M. Kishinevskii and E. S. Parilis, *Izv. Akad. Nauk SSSR, Ser. Fiz.* **26**, 1415 (1962) [*Bull. Acad. Sci. USSR, Phys. Ser.* **26**, 1432 (1962)].
- ²⁶E. V. Alonso, R. A. Baragiola, J. Ferrón, and A. Oliva Florio (unpublished).
- ²⁷N. Benazeth, C. Benazeth, and L. Viel, *Abstracts of the Seventh International Conference on Atomic Collisions in Solids* (Moscow State University, Moscow, 1977), p. 351.
- ²⁸O. Hachenberg and W. Brauer, in *Advances in Electronics and Electron Physics*, edited by L. Marton (Academic, New York, 1959), Vol. XI, p. 413.
- ²⁹I. Adawi, *Phys. Rev.* **134**, A1649 (1964).
- ³⁰R. A. Lowry and G. H. Miller, *Phys. Rev.* **109**, 826 (1958); J. A. Phipps, J. W. Boring, and R. A. Lowry, *ibid.* **135**, A36 (1964); J. W. Boring, G. E. Strohl, and F. R. Woods, *ibid.* **140**, A1065 (1965).
- ³¹J. J. Quinn, *Phys. Rev.* **126**, 1453 (1962); *Appl. Phys. Lett.* **2**, 167 (1963); S. L. Adler, *Phys. Rev.* **130**, 1654 (1963).
- ³²J. C. Ashley, C. J. Tung, R. H. Ritchie, and V. E. Anderson, *IEEE Trans. Nucl. Sci.* **NS-23**, 1833 (1976) and references therein.
- ³³H. Bruining, *Physics and Applications of Secondary Electron Emission* (Pergamon, London, 1954), Chap. VI.
- ³⁴R. M. More, *Phys. Rev. B* **9**, 392 (1974).
- ³⁵R. G. Lye and A. J. Dekker, *Phys. Rev.* **107**, 977 (1957).
- ³⁶S. Thomas and E. B. Pattinson, *J. Phys. D* **3**, 349 (1970), and references therein.
- ³⁷H. A. Bethe, *Phys. Rev.* **59**, 940 (1941).
- ³⁸E. J. Sternglass, *Phys. Rev.* **108**, 1 (1957).
- ³⁹H. H. Andersen and J. F. Ziegler, *Hydrogen Stopping Powers and Ranges in All Elements* (Pergamon, New York, 1977).
- ⁴⁰R. J. Beuhler and L. Friedman, *J. Appl. Phys.* **48**, 3928 (1977).